SF2A 2011
G. Alecian, K. Belkacem, R. Samadi and D. Valls-Gabaud (eds)

INFRARED EXCESS AND EXTENDED EMISSION AROUND CEPHEIDS

A. Gallenne[1], P. Kervella[1] and A. Mérand[2]

Abstract. We present new thermal IR photometry and spectral energy distributions (SEDs) of the classical Cepheids W Sgr, Y Oph and FF Aql, using newly obtained *VISIR* thermal IR photometric measurements. We used the BURST mode of the instrument to get diffraction-limited images at 8.59, 11.25 and 11.85 μm. For these three stars, the SEDs show an IR excess at long wavelengths. These excesses are likely extended emissions surrounding the stars linked to a possible mass loss mechanism. We also detected a spatially extended emission around W Sgr and Y Oph while we do not resolve the circumstellar envelope of FF Aql.

Keywords: Stars: circumstellar matter, Stars: variables: Cepheids, Infrared: stars

1 Introduction

The discovery of circumstellar envelopes (CSEs) around several Galactic Cepheids is an indication that many Cepheids, if not all, are surrounded by CSEs. These CSEs have an effect on the infrared surface brightness technique (IRSB) since the Cepheid appears brighter and also on interferometric measurements since the star appears larger than it really is. It is therefore necessary to quantify this excess in order to estimate the bias on the distance. This circumstellar material is also important in the context of Cepheid mass-loss since it may play a significant role in the problem of the Cepheid mass discrepancy (see e.g. Neilson et al. 2010a). The infrared excess could be linked to a mass-loss mechanism generated by shocks between different layers of the Cepheid's atmosphere during the pulsation cycle. A correlation between the period and the envelope flux (relatively to the star) was proposed by Mérand et al. (2007). A Cepheid with a larger pulsation period would have a larger IR excess. On the other hand, from photometry on a larger sample of Cepheids, Neilson et al. (2010b) reach the opposite conclusion. It is thus essential to study these CSEs to quantify their contribution and to understand how they form.

We present new observations of three Classical Cepheids, W Sgr, Y Oph and FF Aql, with the *VISIR* instrument from the VLT. We present the data analysis using aperture photometry applied to our images and we study the spectral energy distribution (SED) of these three stars. We also look for a spatially resolved component using a Fourier technique analysis.

2 Observation and data reduction

The observations were carried out during May 2008 using the BURST mode of *VISIR* to obtain the best spatial resolution. Series of observations were obtained in three filters: PAH1, PAH2 and SiC (respectively $8.59 \pm 0.42\,\mu$m, $11.25 \pm 0.59\,\mu$m and $11.85 \pm 2.34\,\mu$m). The classical chopping–nodding technique was applied to correct for instrumental artefacts and background thermal emission.

Our first step in the data reduction process consisted of a classical subtraction of the chopped and nodded images in order to remove the thermal background and in storing them in data cubes that contain thousands of frames. To have the best diffraction-limited images, we selected 50 % of the best frames according to the brightest pixel (as tracer of the Strehl ratio). We then proceeded to a precentering (at a integer pixel level), a spatial resampling by a factor of 4 using a cubic spline interpolation and a fine recentering using a Gaussian

[1] LESIA, Observatoire de Paris, CNRS UMR 8109, UPMC, Université Paris Diderot, 5 Place Jules Janssen, F-92195 Meudon, France
[2] European Southern Observatory, Alonso de Córdova 3107, Casilla 19001, Santiago 19, Chile

fitting (at a precision level of a few milliarcseconds). The resulting cubes were then averaged to get the final image used in the data analysis process. This raw data processing has already been used and has proven its efficiency (see e.g. Kervella & Domiciano de Souza 2007; Kervella et al. 2009; Gallenne et al. 2011). The efficiency of the cube mode vs. the standard long exposure mode is discussed in Kervella & Domiciano de Souza (2007).

3 Spectral energy distribution

We carried out a classical aperture photometry on our final average images to assess the flux density for each star in each filter. Photometric templates from Cohen et al. (1999) were used to have an absolute calibration of the flux density, taking into account the filter transmission and the airmass correction from Schütz & Sterzik (2005). We have then collected additional photometric measurements from $0.4\,\mu$m to $100\,\mu$m to analyse the spectral energy distribution of our Cepheids.

As they are pulsating stars, the SEDs vary during the pulsation cycle and we have to take into account the phase of pulsation when retrieving the data. To estimate the magnitudes at our phase of pulsation we retrieved the B, V, J, H and K light curves from the literature when available, that we plotted as a function of phase. We then applied the Fourier decomposition technique (see e.g. Ngeow et al. 2003) to estimate the value at our phase. At longer wavelength, there are no existing light curves, we then chose to use the amplitude of the light curves A_λ (that is decreasing with wavelengths) as additional uncertainties on the magnitude due to the phase mismatch. Based on the estimated J, H and K amplitudes of 51 Galactic Cepheids from Laney & Stobie (1993), we chose as additional uncertainties on the magnitude for $1 < \lambda < 3.5\,\mu$m, the values 0.1 mag for W Sgr and FF Aql and 0.2 mag for Y Oph, and for $\lambda > 3.5\,\mu$m we chose 0.05 mag for the three stars.

The photospheric emission was modelled with tabulated stellar atmosphere models obtained with the ATLAS9 simulation code from Castelli & Kurucz (2003). We have chosen a grid which was computed for solar metallicity and a turbulence velocity of $2\,\mathrm{km\,s^{-1}}$. We then interpolated this grid in order to compute spectra for any effective temperature and any surface gravity. The spectrum was multiplied by the solid angle of the stellar photosphere, $\pi\theta_{\rm LD}^2/4$, where $\theta_{\rm LD}$ is the limb-darkened angular diameter. We adjusted the photometric data to the model taking into account the spectral response of each instrument. We assume that there is no detectable excess (5 % or less) below $2.2\,\mu$m and all the photometric measurements bluer than the K band are used to fit the angular diameter and the effective temperature.

All flux densities $< 3\,\mu$m are corrected for interstellar extinction $A_\lambda = R_\lambda\,E(B-V)$ using the total-to-selective absorption ratios R_λ from Fouqué et al. (2003) and Hindsley & Bell (1989), and the color excess $E(B-V)$ from Fouqué et al. (2007). Fluxes in any other longer wavelengths are not corrected for the interstellar extinction, which we assume to be negligible.

3.1 FF Aql

We selected $\log g = 2.05$ from Luck et al. (2008) as fixed parameter. The adjusted SED is presented in Fig. 1. The B and V values were taken from light curves of Berdnikov (2008) and Moffett & Barnes (1984). The J, H and Ks photometry are from Welch et al. (1984). We also added photometric values from the Infrared Array Camera (*IRAC*: 3.6, 4.5, 5.8 and $8\,\mu$m) and the Multiband Imaging Photometer (*MIPS*: $24\,\mu$m) installed in the *Spitzer* space telescope (Marengo et al. 2010). We also use broadband photometry from the Infrared Astronomical Satellite (*IRAS*: 12 and $25\,\mu$m, Helou & Walker 1988), from the *AKARI* satellite *IRC* point source catalogue (9 and $18\,\mu$m, Ishihara et al. 2010) and from the Midcourse Space Experiment (*MSX*: 8.28, 12.13, 14.65, 21.34 μm, Egan & Price 1996; Egan et al. 2003).

0ur best-fit values are $\theta_{\rm LD} = 0.86 \pm 0.03$ mas and $T_{\rm eff} = 5890 \pm 235$ K. The SED is plotted in Fig. 1 (black solid curve). This fitted effective temperature is only 3 % smaller than the value from Luck et al. (2008) (6062 ± 43 K) at this phase of pulsation. The angular diameter is in excellent agreement with the 0.86 ± 0.17 mas from Groenewegen (2007).

We fitted to this star a second component assuming it follows a simple greybody distribution of the form :

$$F_\lambda = \beta\, B_\lambda(T_{\rm d})$$

where $B_\lambda(T_{\rm d})$ is the Planck function at dust temperature $T_{\rm d}$ and β contains the informations about the solid angle and the total emissivity. Our best greybody model with a temperature $T_{\rm d} = 556 \pm 177$ K and $\beta = 1.50 \pm 0.54\,\mathrm{mas}^2$ is plotted in Fig. 1 (the solid green curve).

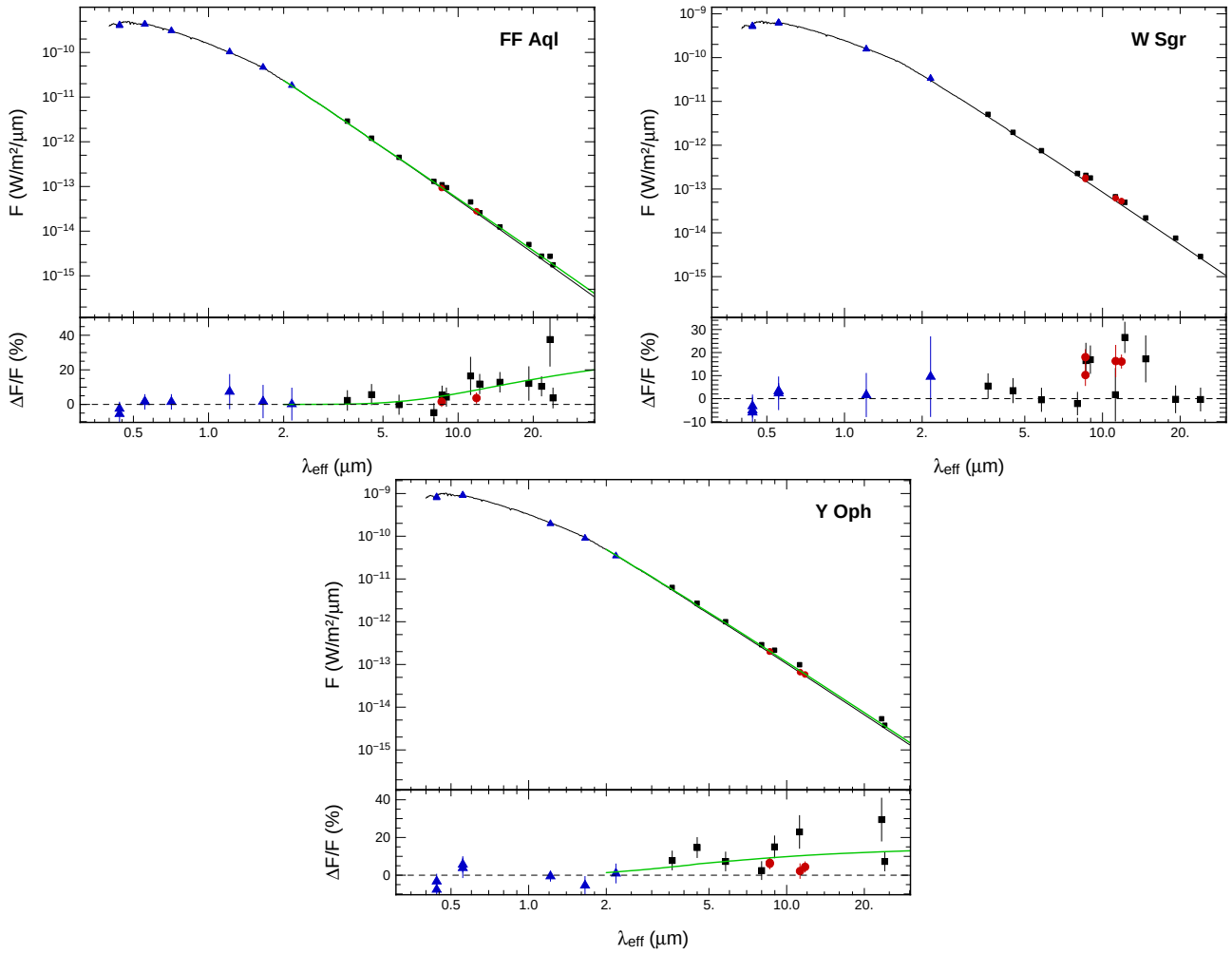

Fig. 1. Synthetic spectra of the classical Cepheid FF Aql, W Sgr and Y Oph (solid line) with the photometric measurements taken from the literature. The blue triangles are the points used to fit the SED. Our measurements are presented with the red circles while the black squares are the other photometric data. On the lower panel is plotted the excess flux density relatively to the photospheric emission. The green curve represents the greybody model.

3.2 W Sgr

The B and V photometry are from Kervella et al. (2004) and Berdnikov (2008). The other irradiances are from *DENIS* (J, Ks), *Spitzer* (3.6, 4.5, 5.8, 8 and 24 μm from Marengo et al. 2010), *IRC* (9 and 18 μm), *MSX* (8.28, 12.13, 14.65, 21.34 μm) and the 12 μm photometry from *IRAS*. The SED is plotted in Fig. 1.

Our fitted effective temperature $T_{\rm eff} = 5623 \pm 162$ K is in agreement at a 2 % level with $T_{\rm eff} = 5535 \pm 51$ K from Luck & Andrievsky (2004) around the same phase with an effective gravity from the same author of 1.7. We found an angular diameter $\theta_{\rm LD} = 1.14 \pm 0.06$ mas that is about 15 % and 1.7σ smaller than the one measured by interferometry by Kervella et al. (2004) (1.31 ± 0.04 mas) at this phase of pulsation. Conversely our estimate is in agreement with the mean diameter from Bersier et al. (1997) who found $\overline{\theta_{\rm LD}} = 1.17 \pm 0.11$ mas based on photometry. However Kervella et al. (2004) used a limb darkened diameter to model their data and the presence of an extended emission could overestimate the angular diameter.

Spitzer's values are consistent with the blackbody radiation adjusted by Marengo et al. (2010). However our *VISIR* photometry shows an excess of ± 15 % . The same trend is observed from IRC (at 9 μm) and *MSX* (at 8.28, 12.13 and 14.65 μm). This could be an evidence of a particular dust composition.

Table 1. Fitted parameters of the $\Psi(\nu, \rho_\lambda, \alpha_\lambda)$ function.

Stars	Filter	ρ ($''$)	α (%)
W Sgr	PAH1	1.14 ± 0.39	3.8 ± 0.6
	PAH2	1.19 ± 0.37	9.1 ± 1.5
	SiC	1.03 ± 0.50	8.3 ± 2.4
Y Oph	PAH1	0.71 ± 0.12	15.1 ± 1.4
	PAH2	1.02 ± 0.52	7.5 ± 2.3
	SiC	0.54 ± 0.46	6.2 ± 4.1

3.3 Y Oph

We retrieved the B, V data from Berdnikov (2008) and Moffett & Barnes (1984). The J, H, K photometry is from Laney & Stoble (1992) and Kervella et al. (2004). The plot of the spectral energy distribution is shown in Fig. 1. The other fluxes are from *Spitzer* (3.6, 4.5, 5.8, 8 and 24 μm from Marengo et al. 2010), *IRC* (9 μm) and the 12 μm and 25 μm photometry from *IRAS*.

The best fitted parameters are $\theta_{\rm LD} = 1.24 \pm 0.05$ mas and $T_{\rm eff} = 5870 \pm 387$ K with $\log g \sim 1.8$ (Luck et al. 2008). Luck et al. (2008) also give an effective temperature at our phase of $T_{\rm eff} = 5800 \pm 148$ K that is in good agreement with our value. Our fitted angular diameter and the value $\theta_{\rm LD} = 1.24 \pm 0.01$ mas measured by Mérand et al. (2007) at this phase of pulsation is also good.

We detected a likely infrared emission from our *VISIR* measurements. This result is consistent with Mérand et al. (2007) where a CSE has been found around this star in the K band with a relative contribution of 5.0 ± 2.0 %. The greybody model of Equ. 3.1 was fitted for wavelengths larger than 3 μm. The best-fitted parameters are $T_{\rm d} = 1009 \pm 183$ K and $\beta = 1.39 \pm 0.23$ mas^2. Y Oph seems to have a hot circumstellar envelope that could be located close to the star and heated by its radiations.

4 Spatially resolved emission

We search for spatially extended emission using a Fourier technique, similar in its principle to the calibration technique used in long baseline interferometry. This method was already used and validated by Kervella et al. (2009); Kervella & Domiciano de Souza (2006). The principle is to divide the Fourier transform modulus of the image of the Cepheid ($I_{\rm cep}$) by that of the calibrator image ($I_{\rm cal}$) to obtain a calibrated visibility function $\Psi(\nu_x, \nu_y)$, with (ν_x, ν_y) denoting the angular spatial frequencies.

We then compute the ring median of Ψ, i.e. the median for a given spatial frequency radius ν over all azimuths (where $\nu^2 = \nu_x^2 + \nu_y^2$). The function $\Psi(\nu)$ obtained is equivalent to a visibility in interferometry. The error bars on Ψ were estimated by the quadratic sum of the dispersion of the PSF calibrator's Fourier modulus over the night and the rms dispersion of the calibrated Ψ function over all azimuth directions for each spatial frequency. A deviation from a central symmetry will not be detected and any departure will be included in the error bars.

Defining a model of a point-like star surrounded by a Gaussian shaped CSE and taking its Fourier transform, it is possible to retrieve the CSE intensity distribution. This type of model was already used by Kervella et al. (2009) and Kervella & Domiciano de Souza (2006) with the $\Psi(\nu)$ function

$$\Psi(\nu, \rho_\lambda, \alpha_\lambda) = \frac{1}{1+\alpha_\lambda}\left[1 + \alpha_\lambda \exp\left(-\frac{(\pi\ \rho_\lambda\ \nu)^2}{4\ln 2}\right)\right]$$

where the Gaussian CSE is defined with a FWHM ρ_λ and a relative flux $\alpha_\lambda = f_{\rm cse}(\lambda)/f_\star(\lambda)$, i.e the ratio of the flux of the envelope to the photospheric flux. We set $V_\star = 1$ since the star is unresolved by *VISIR*.

We applied the fit using a classical χ^2 minimization to all the final images. We did not detect spatially resolved emission for FF Aql. For W Sgr and Y Oph that show a resolved component, the fitted parameters are presented in Table 1 with the Ψ function plotted in Fig. 2.

For FF Aql, an upper limit of ~ 265 mas can be set for the extension of the CSE based on the telescope resolution.

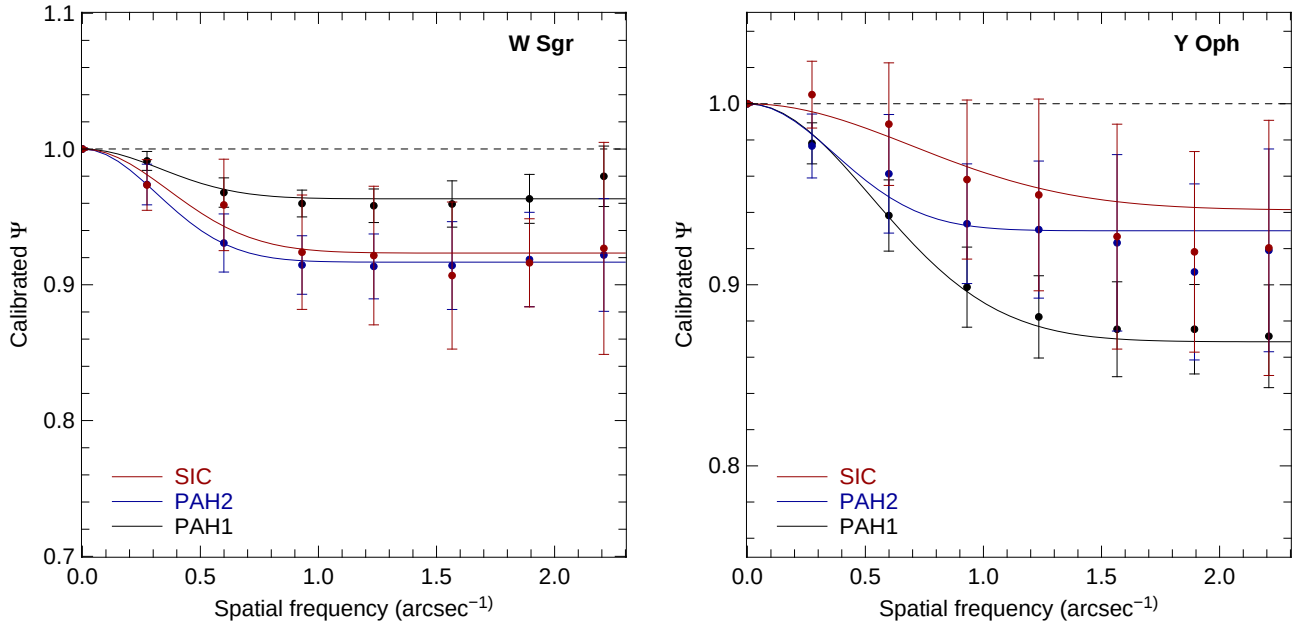

Fig. 2. Fit of a Gaussian CSE + unresolved point source model to the Ψ functions of our Cepheids. The dashed curve is here for a reference as an unresolved star.

5 Conclusions

We presented new thermal IR photometry and spectral energy distributions of 3 classical Cepheids. We detected infrared excess around all of them. This confirms that the presence of circumstellar material around Classical Cepheids is a widespread phenomenon. The origin of these CSEs is not well understood. Their presence could be linked to mass loss from the star. It has been suggested that the IR excess is caused by dust formed in a wind from the Cepheids (Kervella et al. 2006). From a radiative-driven wind model including pulsation and shock effects Neilson & Lester (2008) concluded that radiative driving is not sufficient to account for the observed IR excesses and proposed that the mass loss could be driven by shocks generated in the atmosphere by the pulsation of the star. Other observational evidences were provided with IR excess detections from *IRAS* observations by Deasy (1988) who estimated mass loss rates ranging from 10^{-10} to $10^{-6}\,M_{\odot}$ yr^{-1}.

Mérand et al. (2007) showed for the classical Cepheids a likely correlation between the pulsation period and the CSE flux (relative to the photosphere) in the K band. We found the same trend at 8.6 μm, in which the longer periods have larger excesses. However a larger sample of Cepheids is needed to confirm this correlation.

The current status of high angular resolution observations indicate that CSEs are present around all Cepheids, and that the brightness of these envelopes is increasing with the pulsation period of the star. The nature of these envelopes is currently unknown. However, several observation techniques, over a broad range of wavelengths, have the potential to bring new informations about their composition and the mechanisms about their creation. For Cepheids, the CSEs represent a potential source of bias for the distance scale. Their contribution in the infrared could significantly affect the calibrations of the Period-Luminosity relations, as they are often based on the infrared surface brightness variant of the Baade-Wesselink method.

We received the support of PHASE, the high angular resolution partnership between ONERA, Observatoire de Paris, CNRS, and University Denis Diderot Paris 7. This work made use of the SIMBAD and VIZIER astrophysical database from CDS, Strasbourg, France and the bibliographic informations from the NASA Astrophysics Data System. Data processing for this work have been done using the Yorick language which is freely available at `http://yorick.sourceforge.net/`. This research is based on observations with AKARI, a JAXA project with the participation of ESA.

References

Berdnikov, L. N. 2008, VizieR Online Data Catalog: II/285, originally published in: Sternberg Astronomical Institute, Moscow, 2285

Bersier, D., Burki, G., & Kurucz, R. L. 1997, A&A, 320, 228

Castelli, F. & Kurucz, R. L. 2003, in IAU Symposium, Uppsala University, Sweden, Vol. 210, Modelling of Stellar Atmospheres, ed. N. Piskunov, W. W. Weiss, & D. F. Gray (ASP), 20

Cohen, M., Walker, R. G., Carter, B., et al. 1999, AJ, 117, 1864

Deasy, H. P. 1988, MNRAS, 231, 673

Egan, M. P. & Price, S. D. 1996, AJ, 112, 2862

Egan, M. P., Price, S. D., Kraemer, K. E., et al. 2003, VizieR Online Data Catalog: V/114. Originally published in: Air Force Research Laboratory Technical Report AFRL-VS-TR-2003-1589 (2003), 5114, 0

Fouqué, P., Arriagada, P., Storm, J., et al. 2007, A&A, 476, 73

Fouqué, P., Storm, J., & Gieren, W. 2003, in Stellar Candles for the Extragalactic Distance Scale, ed. D. Alloin & W. Gieren, Vol. 635, 21–44

Gallenne, A., Mérand, A., Kervella, P., & Girard, J. H. V. 2011, A&A, 527, A51

Groenewegen, M. A. T. 2007, A&A, 474, 975

Helou, G. & Walker, D. W., eds. 1988, IRAS catalogue, Vol. 7 (STI)

Hindsley, R. B. & Bell, R. A. 1989, ApJ, 341, 1004

Ishihara, D., Onaka, T., Kataza, H., et al. 2010, A&A, 514, A1

Kervella, P., Bersier, D., Mourard, D., et al. 2004, A&A, 428, 587

Kervella, P. & Domiciano de Souza, A. 2006, A&A, 453, 1059

Kervella, P. & Domiciano de Souza, A. 2007, A&A, 474, L49

Kervella, P., Mérand, A., & Gallenne, A. 2009, A&A, 498, 425

Kervella, P., Mérand, A., Perrin, G., & Coudé Du Foresto, V. 2006, A&A, 448, 623

Laney, C. D. & Stobie, R. S. 1993, MNRAS, 260, 408

Laney, C. D. & Stoble, R. S. 1992, A&AS, 93, 93

Luck, R. E. & Andrievsky, S. M. 2004, AJ, 128, 343

Luck, R. E., Andrievsky, S. M., Fokin, A., & Kovtyukh, V. V. 2008, AJ, 136, 98

Marengo, M., Evans, N. R., Barmby, P., et al. 2010, ApJ, 709, 120

Mérand, A., Aufdenberg, J. P., Kervella, P., et al. 2007, ApJ, 664, 1093

Moffett, T. J. & Barnes, III, T. G. 1984, ApJS, 55, 389

Neilson, H. R., Cantiello, M., & Langer, N. 2010a, ArXiv e-prints

Neilson, H. R. & Lester, J. B. 2008, ApJ, 684, 569

Neilson, H. R., Ngeow, C., Kanbur, S. M., & Lester, J. B. 2010b, ApJ, 716, 1136

Ngeow, C., Kanbur, S. M., Nikolaev, S., Tanvir, N. R., & Hendry, M. A. 2003, ApJ, 586, 959

Schütz, O. & Sterzik, M. 2005, in High Resolution Infrared Spectroscopy in Astronomy, ed. H. U. Käufl, R. Siebenmorgen, & A. Moorwood, Proceedings of an ESO Workshop held at Garching, Germany, 104–108

Welch, D. L., Wieland, F., McAlary, C. W., et al. 1984, ApJS, 54, 547